

Nano or micro grained alumina powder? A choose before sintering

R. ROMÁN, T. HERNÁNDEZ, and M. GONZÁLEZ

CIEMAT-FNL.
Madrid, Spain.

Two different wet routes have been used to synthesize alumina powders in order to compare the characteristics of the final product and its behaviour during sintering. The Homogeneous Precipitation (HP) gives rise to nanoparticulated powders of about 2 nm. However, such particles quickly aggregate and grow with calcination temperature. The Polymerized Organic-Inorganic Synthesis (POI) produces homogeneous particle size powders (about 1 micron) after resin charring. The characterization of the powder surface is the basis of an efficient process control. Particle characterization parameters (morphology, crystallinity and degree of aggregation) are characterized by different techniques, such as DTA/TG, IR, XRD, SEM and TEM, and compared between these synthesis methods. The results show the evolution from the amorphous to the corundum alumina phase for both processes and their ability for sintering, as well discusses the beneficial of nanoparticles obtained by HP during sintering.

Keywords: alumina, synthesis, nanoparticles, homogeneous precipitation, PVA.

¿Nano o micro polvos de alúmina? Una elección antes de la sinterización

Se han utilizado dos diferentes síntesis por vía húmeda para la preparación de polvos de alúmina con el fin de comparar las características de los productos finales y su comportamiento durante la sinterización. La Precipitación Homogénea (HP) da lugar a polvos nanoparticulados de unos 2nm. Se observa sin embargo, como estas partículas se agregan rápidamente y crecen con la temperatura de calcinación. La Síntesis por Polimerización Orgánica-Inorgánica (POI) produce polvos de tamaño de partícula homogéneo (en torno a 1 micra) después de la descomposición de la resina. La caracterización de la superficie de los polvos es la base de un control eficiente del proceso. Los parámetros de caracterización de las partículas obtenidas (morfolología, cristalinidad y grado de agregación) se obtienen por diferentes técnicas como DTA/TG, IR, XRD, SEM y TEM, y se comparan entre estos métodos de síntesis. Los resultados muestran la evolución desde el amorfo a la fase de corindón de la alúmina para ambos procesos y su capacidad para la sinterización.

Palabras clave: alúmina, síntesis, nanopartículas, precipitación homogénea, PVA.

1. INTRODUCTION

An important aspect of nanotechnology is the development of synthesis protocols for realizing nanomaterials over a range of sizes, shapes and chemical compositions. The synthesis strategy of nanoparticles and nanomaterials accommodate precursors from liquid, solid or gas phase and the methods can be divided into three main groups: synthesis of particles from the solution of the corresponding salts by controlled addition of ions, hydrolysis (1), thermal decomposition, or synthesis in aerosols (2).

Alumina is an advanced ceramic with excellent chemical, thermomechanical and dielectrical properties. It makes this oxide an excellent material for structural, microelectronic and technological applications, from bioceramics implants to electrical insulators inside the thermonuclear fusion reactors (3). Fabrication of nanometric alumina powders is being developed due to the improved properties related to

smaller particle size, and higher specific surface areas. Papers concerning the obtention of alumina from gels are found in the literature (4).

Ceramics are usually manufactured by conventional processes (mechanically processing of oxides and/or carbonates followed by calcination and milling), which are inadequate for many advanced applications. Problems arise with the poor sintering behaviour and inhomogeneity, as a result of large and strongly bonded powder agglomerates. In order to solve these difficulties, there is an increasing interest in alternative synthetic routes (5), (6), (7) for several reasons. First, chemical impurities have a detrimental effect on the high-temperature mechanical behaviour of engineering ceramics and on the electrical properties of electroceramics (8) so that greater purity derived from novel synthesis can lead to improved physical properties. Secondly, conventional routes

are not versatile for producing a wide range of coatings and fibrous materials. The obtention of alumina nanopowders has been usually focused to improve its optical properties (9). Non-uniform powders make difficult a reproducible manufacture of components because of chemical inhomogeneity and voids produced in the microstructure. Hence, powders with physical characteristics that allow reliable fabrication are required.

Usually, the method of arrested precipitation results in a non-uniform size distribution of nanoparticles, however the hydrolysis of inorganic salts represents a promising method for the synthesis of materials with a variety of properties and application in novel electric, magnetic and optic devices. This method, also named as Homogeneous Precipitation (HP) (10), is based on the thermal instability of some organic alkalis (i.e. urea) with the increase of temperature and solution acidification. In such conditions urea is hydrolysed and the released NH_3 causes the subsequent hydrolysis of the metal salts present in the solution. Although the obtained nanocrystalline oxides offer exciting technological possibilities, they suffer grain growth and particle coarsening at relatively moderate temperatures with the subsequent loss of nanocrystalline behaviour (11).

On the other hand, the Polymerized Organic-Inorganic synthesis (POI) is a useful and rather simple way to obtain homogeneous powders. It makes use of a polyhydroxylated linear polymer soluble in water in all proportions (12,13), being the polyvinyl alcohol (PVA) the most used polymer. When an aqueous solution containing cationic salts and small quantities of PVA is evaporated, solution viscosity increases until eventually it becomes a gel. The cation species get entrapped inside the polymer network structure. Since salt decomposition and water boiling produce bubbles inside the gel, a foam is formed which gives rise to an amorphous xerogel upon calcination.

There is difficult to find papers related to the ability of nanometric alumina to sinter. This work reports on the synthesis of particulated powders by the previously described HP and POI chemical routes as an alumina ceramic precursor. The synthesized materials are analyzed by IR spectroscopy, TG/DTA, X-Ray diffraction and electron microscopy, and powders processability is discussed on the basis of the obtained results. The dynamic sintering supplies relevant information about the quality of the final dense bodies..

2. EXPERIMENTAL

2.1. Synthesis and sintering of alumina powders

Using the HP method, a colloidal suspension was obtained by mixing an aqueous solution containing $0.0075 \text{ mole} \times \text{dm}^{-3}$ of aluminium nitrate ($\text{Al}(\text{NO}_3)_3 \cdot 9\text{H}_2\text{O}$, extra pure, Merck) with $0.1 \text{ mole} \times \text{dm}^{-3}$ of Urea (Probos) to induce precipitation. The starting solution was aged at 60°C for 400 h to evaporate the excess of water up to the precipitation of a glassy gel. The evolution was monitored by measuring the pH of the suspension. The gel was later dehydrated at 100°C . Finally, the dried precipitate was divided into several parts and calcined from 350°C to 1200°C during 2 h. These samples will be hereafter named as "H".

Aqueous solutions of aluminium nitrate and polyvinyl alcohol (PVA, Fluka) were used when following the POI synthesis method. The reactive proportion was calculated

according to the results of Gulgun et al. (14), where the ratio of positive charges due to Al^{3+} cations to the PVA monomer should be 4:1. The degree of polymerization of PVA used has a value of 1600 (monomers/polymer). The $\text{Al}(\text{NO}_3)_3$ solution was slowly added to the PVA in order to avoid an excessive foam formation. To assure a good homogeneity the mixed was stirred and simultaneously heated at 85°C to eliminate the excess of water and nitric acid. The viscosity of the mixture progressively increases until the formation of a gel. The resulting gel-type precursor was then heated at 200°C , obtaining a yellow resin that finally was divided in several fractions and calcined from 350°C to 1200°C during 2 h. These samples will be named as "P".

In order to examine the sintering behaviour of both alumina powders, the 1200°C calcined powders were then attrition milled in ethanol, dried, sieved and isostatic pressed at 200 MPa. The pressed bodies were then presintered at 1300°C for 4 h, cut into disks of 20 mm in diameter and 3 mm thickness and finally sintered at 1600°C for 2 h.

2.2. Characterization Methods

The pH evolution of the HP solution was measured using a precision compact pHmeter (InoLab pH Level 2, WTW GmbH).

The colloidal particle size of the HP emulsion and the dried powders were measured at room temperature by Photon Correlation Spectroscopy (PCS), using a 500 mW Argon laser particle size analyzer (model 4700, Malvern) working with a wavelength of 514 nm.

The precursors into oxide conversion and the formation of different crystalline phases were followed by thermogravimetry and differential thermal analysis using a Seiko TG/DTA 6300 equipment. The tests were carried out under air atmosphere from room temperature to 1200°C at a heating rate of $10^\circ\text{C min}^{-1}$. This evolution was also followed by infrared spectroscopy, employing a Nicolet 5700 IR spectrometer in the range of $4000\text{--}400 \text{ cm}^{-1}$ and using a smart performer single-reflection ATR Accessory. The crystalline evolution as a function of calcination temperature was analyzed by X-Ray diffraction using a Philips diffractometer X-Pert-MPD with $\text{CuK}\alpha$ radiation and Si monochromator. The apparent bulk densities of the sintered samples were measured using the mass and dimensions method. Relative density was calculated using pure alumina as a reference.

The morphology of gel precursors was observed using a transmission electron microscope equipped with an X-Ray Dispersive Energy analyzer TEM-EDX (Philips CM200FEG) working at 200 kV with a $2,35 \text{ \AA}$ structural resolution. The morphology of calcined particles and the microstructure of the sintered ceramics were studied by scanning electron microscopy using a SEM, Hitachi S-2500 at 25 kV. For microstructural examination, the sintered specimens were ground, polished down to a $1 \mu\text{m}$ diamond finish and thermally etched during 30 min at temperature 25°C below sintering temperature to reveal the grain boundaries.

The shrinkage signal ΔL or the CTE value (coefficient of thermal expansion) was measured over temperature up to 1650°C to know the ability to sinter for each powder. The equipment was a Dilatometer Linseis L75H from room temperature to 1625°C . Data were recorded every two grades.

3. RESULTS

3.1. Obtention of nanoparticulated gels and their thermal behaviour

3.1.1. Synthesis of the HP precursor

During the HP solution aging at 60 °C, a dramatic change of pH from 3.9 to 7.5 is observed between 150 and 250 h (fig. 1). This pH variation is due to the slow urea decomposition and the subsequent colloidal precipitation. It is important to notice that when the system reaches a basic pH, the colloidal solution remains stable even after several months. The gel obtained by this route is formed by small microaggregates

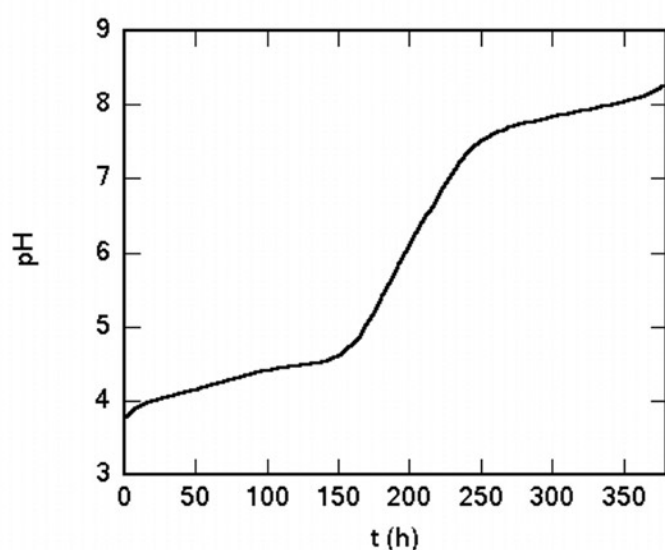
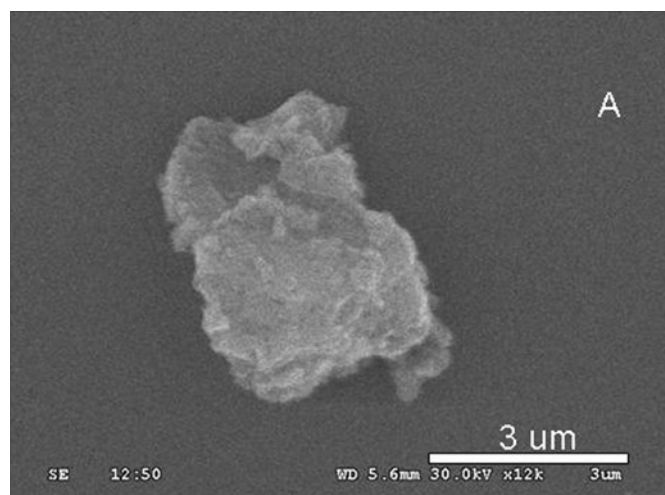


Fig. 1- pH evolution with ageing time of the HP solution.



of particles of few nanometers, as can be observed in the SEM and TEM micrographs of figure 2. The gel thermal evolution when increasing temperature is shown in figure 3. An endothermic peak below 100 °C is indicating the elimination of the absorbed water. The weight loss due to this effect was calculated to be the 4%. The most important loss of weight occurs from 100 °C to 400 °C (about an 80%) which can be associated to a continuous dehydration with loss of the chemically bonded water. This is reflected in the DTA curve by the endothermic peaks located at 220 °C and 270 °C. The transition from the aluminium hydrates to ordered alumina phases is associated to the exothermic peaks found at 300 °C and 450 °C. From this temperature any more weight losses are noticed. However other structural changes are observed at 800 °C and 1075 °C, which may be related with the initial formation of gamma and alpha alumina phases, as will be demonstrated below.

3.1.2. Synthesis following the POI method

During this synthesis method, it was necessary to heat up to 85 °C to produce the viscosity increase of the initial transparent solution and to develop into a yellowish gel. Moreover, any precipitation was observed at temperatures below 200 °C. After applying 200 °C for 20 h, the gel becomes an aerogel that finally transforms into a white spongy ash when temperature is increased up to 350 °C. The thermal behaviour is very similar to that of the P precursor. As can be observed in figure 3b, the DTA analysis shows that most of the volatile and organic compounds are eliminated at temperatures below 400 °C. The unreacted PVA and the excess of water are completely removed at about 200 °C, as it is shown from the endothermic peaks registered at this temperature range. The weight loss at 200 °C of a 56.7 % is revealed in the TG curve and also corresponds to the polymer

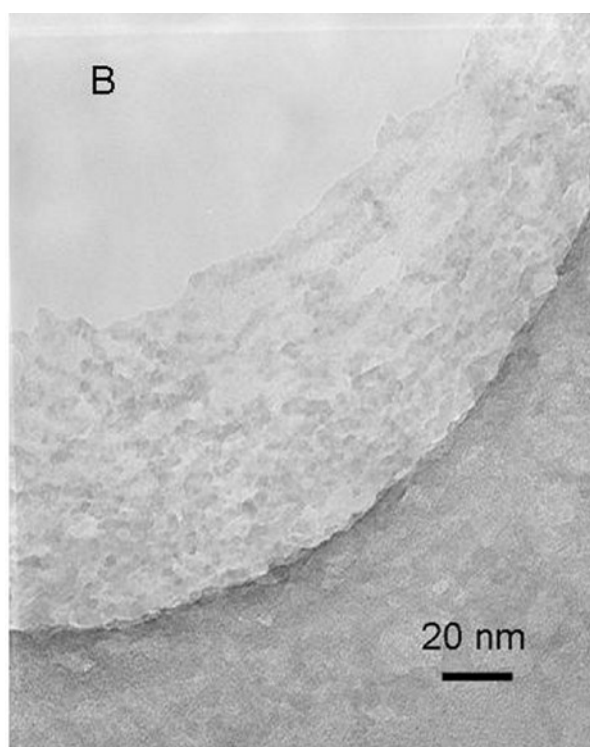


Fig. 2- (A) SEM image of the P agglomerates obtained after the resin charring (POI method) and (B) TEM micrograph showing the gel morphology obtained by the precipitation method.

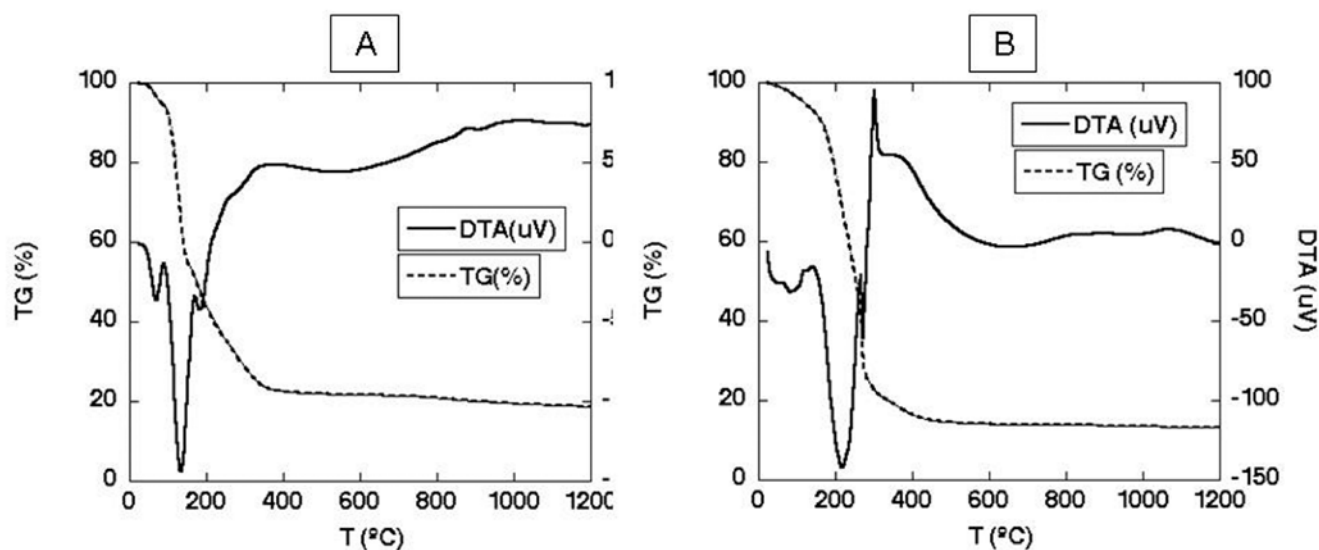


Fig. 3- TG and DTA curves registered during (A) P xerogel and (B) H powder thermal decomposition.

condensation that occurs simultaneously to the water loss. The polymer and nitrates decomposition takes place from 200 °C to 800 °C in a continuous process with overlapped steps. This temperature range is characterised by a broad exothermic band associated to a weight loss of a 22.7 %. Exceeding this temperature, the weight loss is noticed anymore although the weak peak in the DTA located at 880 °C could be indicating the gamma alumina nucleation.

3.2. Crystal Evolution

The chemical surface character was analyzed by means of an IR beam in contact with the calcined powders, allowing the study of oxide formation from the organic intermediates during synthesis and processing. The evolution of IR spectra

with calcination temperature of both synthesized gels is plotted in figure 4. The spectra show a very similar behaviour on both materials. Up to 850 °C, only the typical frequencies of AlO_4 tetrahedra (15) are registered. In the 500 cm^{-1} region, vibrations may be due to some bending motion of the AlO_4 lattice. On both plots, the typical pattern of the gamma phase is easily identified at any calcination temperature with the exception of 1200 °C. However, the change in the tendency at 850 °C on the P powders could be already indicating the presence of the emerging alpha phase. The wide band corresponding to the Al-O bonds for the transition aluminas develops into two or three small bands at 750, 570 and 460 cm^{-1} when temperature is increased to 1200 °C. The corundum structure is built up only on octahedral AlO_6 and the most characteristic IR feature is the occurrence of two strong bands near 650 and 600 cm^{-1} together

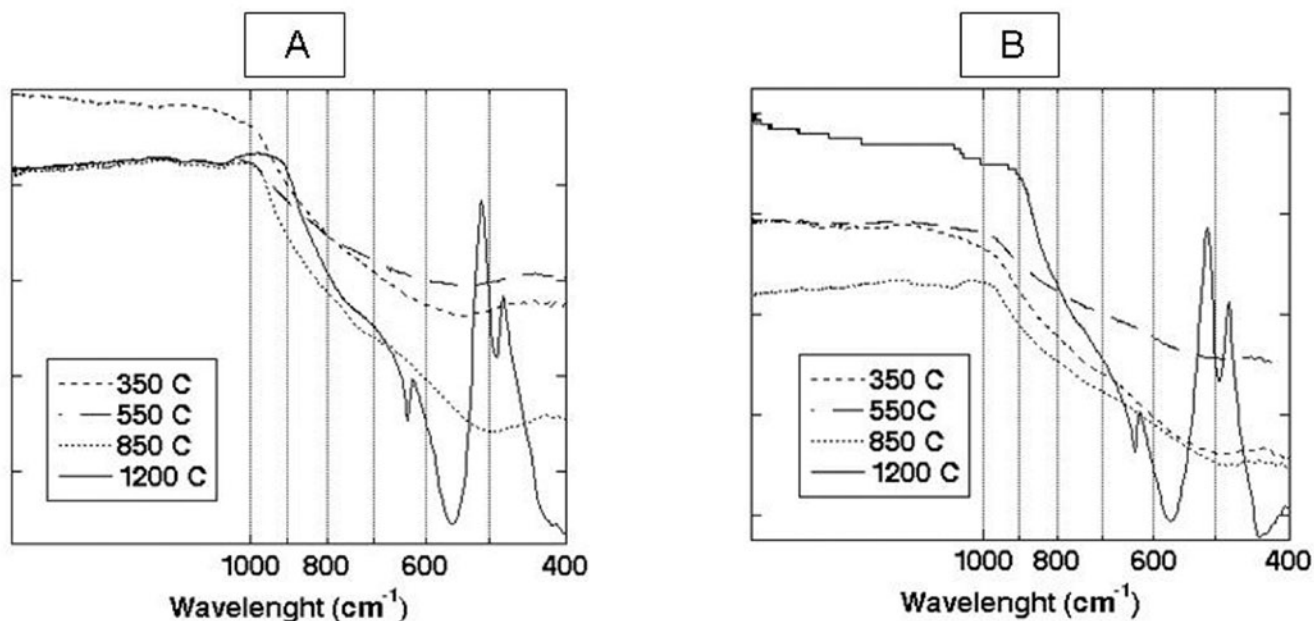


Fig. 4- IR-spectra as a function of calcination temperature of powders obtained from (a) POI gels and (b) HP synthesis.

with some others of less intensity around 450 and 480 cm^{-1} .

The XRD patterns as a function of the temperature show a quasi-amorphous phase at heating temperatures of 350 and 550 °C (fig. 5). The most important difference between the synthesis processes appears at 850 °C. At this temperature, only the gamma alumina phase is presented on the H sample. However, the P diffraction pattern reveals that both gamma and alpha alumina phases are coexisting, although the former is the main crystal structure. The same result can be appreciated by studying the IR spectra, in which the wide band corresponding to the low coordination aluminium begins to define into sharper bands at 850 °C in the case of the P sample, but it is not observed in the IR curve corresponding to H powders.

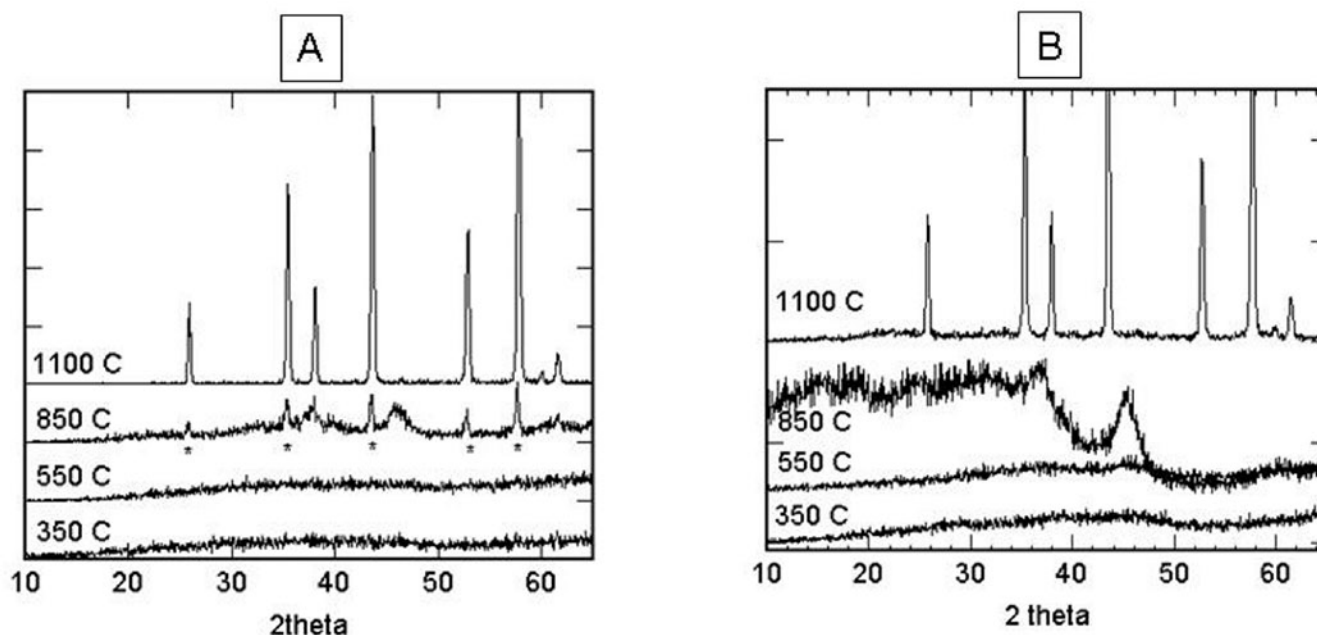


Fig. 5- XRD patterns at different calcination temperatures of samples obtained through (a) the POI and (b) the HP synthesis routes. Alpha phase is marked with an asterisk.

3.3. Powder Microstructure and Particle Size

Comparing the two synthesis processes, it must be pointed out the moment at which the primary particles are obtained. The evolution of particle size with heating temperature is shown in table I. Just at 60 °C, the homogeneous precipitation produces very small particles of about 2-5 nm (see fig. 2a), however, during drying, such particles develop into hard agglomerates. In the POI method the aerogel charring begins about 300 °C but is not completed up to higher temperatures since the pyrolysis produces carbon-wastes in the powder that need temperatures close to 1000 °C to be eliminated. For such

TABLE I. GRAIN SIZE OF THE SAMPLES HEATED AT DIFFERENT TEMPERATURES

Sample	Heat treatment	Particle size (nm)	Error
H	As obtained	5	± 2
H	Aged during 400 h	482	± 86
H	850 °C	520	± 12
H	1200 °C	> 3000	-
P	1200 °C	1238	± 156

reason particle size could not be measured up to 1200 °C, when all the organics and its thermal derivatives were eliminated and not interfering in the particle size measure. This temperature provokes the starting amorphous POI agglomerates of about 3 micron in size (fig. 2b). As an example, figures 6a and 6b show the particle morphology and agglomerates size of the synthesized powders heated at 1200 °C, at which temperature the corundum phase is fully formed. The inset of figure 6b shows that the single particle of the H sample is about the half of the P sample (200 nm and 400 nm, respectively). Nevertheless during calcination, the P particles agglomerate softly and more homogeneously than the H ones and can be easily broken into single particles by milling.

3.4. Dynamic Sintering

The shrinkage (dL/L_0) of the discs during heating of both materials is plotted in the figure 7, as well as the kinetic (α) of the processes. It can be noticed the differences between their behaviour. Since the P sample begins to reduce over 1200 °C and is a continuous and slow progression, the shrinkage for H is noticeable about 700 °C and the sintering occurs by means a multistep process at two ranges of temperatures: 900-1100 °C and over 1400 °C. It is important to consider that the sintering is not finished neither, H nor P, for 1625 °C. Technical limitations prevented to track the tests over such temperature, but it is clear that for the P sample the end of the shrinkage could be quite far. Anyway, the H sample sintering behaviour seem to be improved respect to the P.

Attending the microstructure changes during heating, the presintered microstructures (fig. 8a and 8b) show clearly that the sintering process is still incipient at 1300 °C. Great agglomerated areas are found along the P microstructure which seems to densify immersed into a matrix of porous alumina. At this temperature, the H sample exhibits grained matrix areas in which the cohesion does not exist. Applying

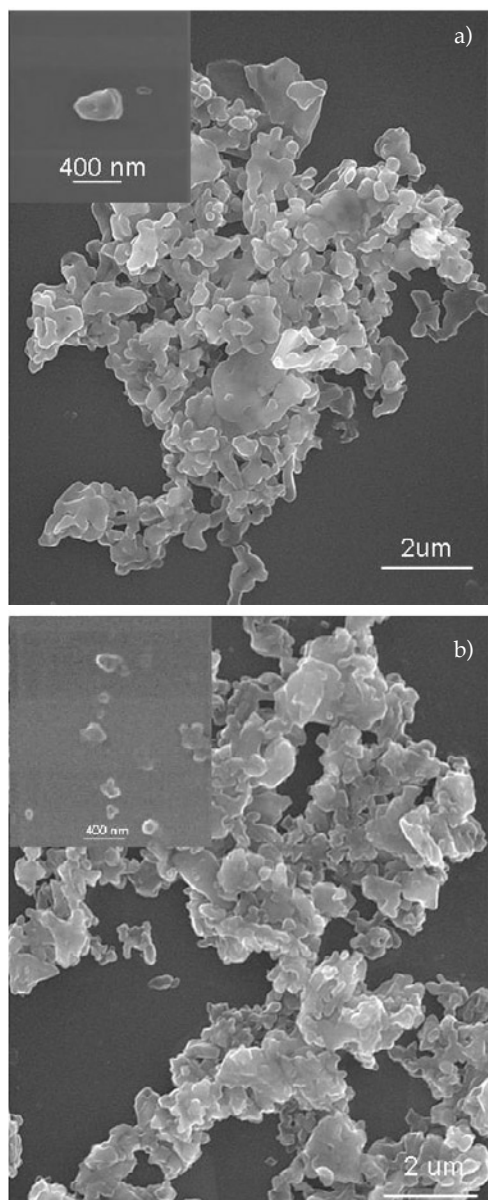


Fig. 6- SEM images of powders synthesized using (a) the POI and (b) the HP synthesis processes after being calcined at 1200 °C. Inlet, singular particles are shown.

1600 °C as the sintering temperature, these microstructures develop toward those shown in figure 8c and 8d. The few big grains found in P material at 1300 °C are now developing into abnormal grown grains (not shown in the figure), although incipient densification has successfully achieved (>91 % alumina theoretical density). On the other hand, the sintering process of the H powder is rather effective, and areas of weak grain binding could be found, while same time, its grain growth is much faster.

4. DISCUSSION

In ceramic processing there is a strong interrelation between the starting raw materials, the powder processing with its sintered microstructure and the quality of the final product. Powder particle parameters (size, shape, morphology,

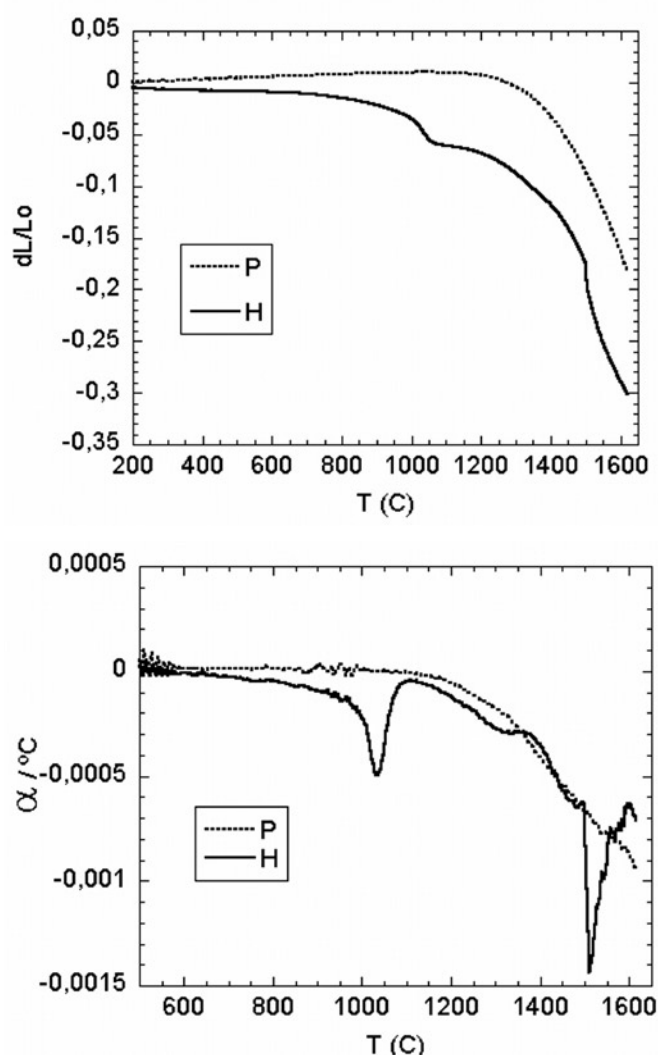


Fig. 7- Shrinkage (dL/L_0) and kinetics (α) vs temperature for the both samples.

degree of agglomeration and agglomerate strength), chemical composition, phase and thermal analysis are used here to obtain relevant data to predict powder behaviour up to the sintering step.

The two methods of synthesis here used successfully produce α -alumina powders. However, each of them presents a number of advantages and disadvantages. It is obvious that the particles surface has a strong impact on the agglomeration of a powder. The interaction between particle surface, solvent and organic additives is one of the most important factors on the quality of a final ceramic product. Homogeneous precipitation provides emulsions formed by nanoparticles that are very stable in time, in fact, it has been verified that once the precipitation step is finished, the suspension keeps stable by at least during six months. The obtained aluminium hydrate could correspond to gibbsite, the reaction takes place at room temperature and according to the data gathered in the published bibliography (16). The H particles are then highly reactive and have a great tendency to agglomerate, even during gel aging. Although the agglomerates in suspension can be easily ultrasonically broken, when dried the bonding forces between particles becomes important and even after aggressive milling the agglomerates remain unaltered. In

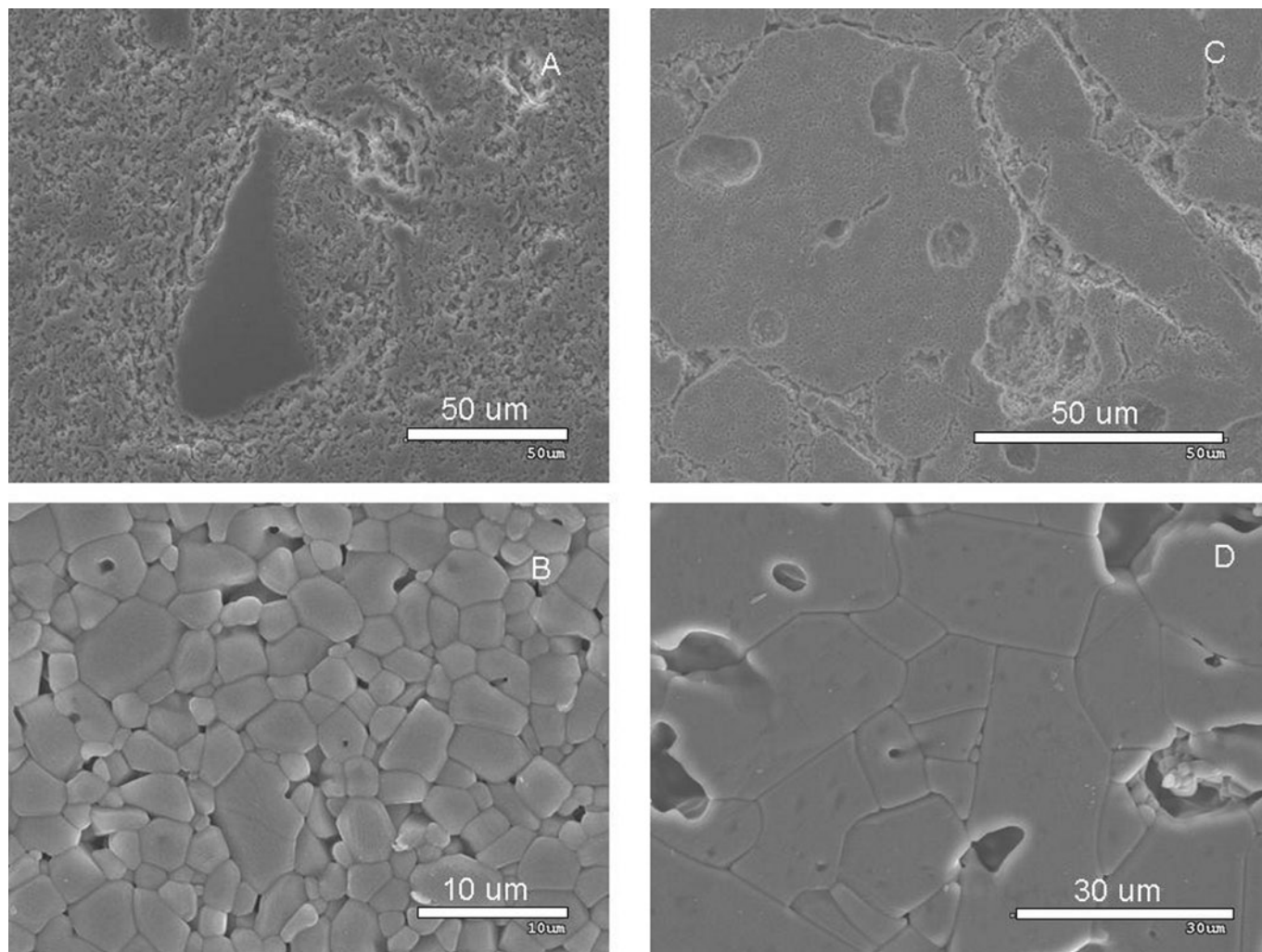


Fig. 8- SEM microstructures of (A) P sample heated at 1300 °C, (B) P sintered at 1600 °C, (C) H sample heated at 1300 °C and (D) H sintered at 1600 °C.

addition and due to the high specific surface area of H gels, there is a high probability of contamination. In term of sinterability, the H powders give rise to a better behaviour, even when harder and big agglomerates have been developed during post-synthesis processing (heat treatments). This means that the original nanoparticles maintain their high reactivity even when they are enclosed into the agglomerates. This elevated reactivity allows the powder to sinter faster and at lower temperatures, although the hard aggregates formed during the precipitate drying of the H precursor were difficult to eliminate by using milling or pressure. However, the study of its microstructure after sintering reveals its poor densification due to void formation between agglomerates, and fast grain growth.

Assuming that size and powder morphology are essential factors for the right packing of particles during powder conformation/processing, and therefore to reach the best densification after sintering, powders obtained by the POI method may behave more suitable than those obtained by the HP synthesis. As shown above, P particles also agglomerate but even after the corundum phase is totally developed the agglomerate size is about three times smaller than that measured on powders obtained by the homogeneous precipitation. However, the POI process mainly produces platelet-like particles that are rigid and difficult to compact by pressing and provokes a poor green density to start the

sintering. In addition, the increase of temperature makes the situation worse and increases the growth of particle bonding and the crystallite coarsening. These observations are in good agreement with Lessing (6), which concludes that the heating schedule during gel setting and calcination affects the final agglomerate morphology of powders obtained via polymeric precursors. Anyway, none of the two used synthesis routes are able to obtain particles which could maintain their nanometric sizes and stable deagglomerated after the heating treatments. Recent studies (17) point out that the degree of polymerization (DP) of the PVA has a great influence on the particle size and on the agglomeration degree of synthesized alumina. So, the use of longer chained PV alcohol (DP value ~1600) on a POI synthesis route will produce synthesized alumina precursors of bigger sized and higher agglomerated particles with respect to PV low-length alcohols (DP ~400).

Comparing the particles obtained by the both methods is evident that in terms of sinterability, the H sample provides a better behaviour than P, even when forms harder and greater agglomerates than those found in the sample P. This means that the original nanoparticles maintain their high reactivity even when are enclosed into the agglomerates and are able to sinter.

From the point of view of sintering, it is evident that the synthesis method determines the future behaviour of the powder (18). Nowadays, several methods are described

to obtain nanoparticulated powders and its utility in technological applications must be assessed. However, the intrinsic characteristics of the nanoparticles make difficult to consider those processes in which high temperatures are required (heat treatments and sintering).

5. CONCLUSIONS

The synthesis method must be carefully chosen considering the final application of the alumina powder. The Homogeneous Precipitation forms very stable suspensions and is an excellent method to provide particles of extremely small size (nanoparticles of about 5 nm). In addition, the amount of the final alumina powder obtained through this route is very little. Therefore, the obtention of alpha-alumina powders in which high processing temperatures are also needed are very time consuming but can give rise to high quality final sintered bodies if the processing route is satisfactory. Nevertheless, it is an excellent synthesis method of stable suspensions of aluminium oxide structures other than corundum phase, and can be useful to prepare nanoparticles for exploring their optical applications such as the chromia-doped alumina materials.

In comparison, the Polymerized Organic-Inorganic synthesis method produces micro and easy to handle particles with little facility of aggregation. Moreover, it is a much faster method, which produces higher amounts of final oxide material. These important characteristics make the POI method very interesting to the synthesis of alumina ceramics, although the polymerization degree and the content of PVA must be controlled to obtain synthesized powders of small particle size and degree of agglomeration.

A better understanding of powder parameters through the use of analytical and surface characterization techniques during both the synthesis and the thermal processing could improve the density and microstructure of sintered alumina ceramics.

ACKNOWLEDGEMENTS

The authors wish to thank Mrs. Montserrat Martin for her technical support during the experimental part of this work.

REFERENCES

1. C. D. Chandler, C. Roger and M. I. H. Smith. Chemical aspects of solution routes to perovskite-phase mixed-metal oxides from metal-organic precursors, *Chem. Rev.* 93, 1205-1241 (1993).
2. P. Murugavel, M. Kalaiselvam, A. R. Raju and C. N. R. Rao. Sub-micrometre spherical particles of TiO_2 , ZrO_2 and PZT by nebulized spray pyrolysis of metal-organic precursors. *J. Mater. Chem.* 7, 1433-1738 (1997).
3. R. Vila, E. R. Hodgson. In-beam dielectric properties of alumina at low frequencies. *J. Nucl. Mater. V.*, 283-287, 903-606 (2000).
4. M. Wakakuwa, A. Makishima and M. Kawashima. Synthesis of gel-derived cellular alumina. *J. Mater. Sci. Letters*, 9, 1304-1306 (1990).
5. M. Radwan, T. Kashiwagi and Y. Miyamoto. New synthesis route for $\text{Si}_3\text{N}_4/\text{O}$ ceramics based on desert sand. *J. Eur. Ceram. Soc.* 23, 13, 2337-2341 (2003).
6. M. Traianidis, C. Courtois and A. Leriche. Mechanism of PZT crystallisation under hydrothermal conditions. Development of a new synthesis route. *J. Eur. Ceram. Soc. V.*, 20 16, 2713-2720 (2000).
7. P. A. Lessing. Mixed-cation oxide powders via polymeric precursors. *Bull. Am. Ceram. Soc. V.*, 68, 1002-1010 (1989).
8. P. Cibor, J. Sedlacek, K. Neufuss. Influence of chemical composition on dielectric properties of Al_2O_3 and ZrO_2 plasma deposits. *Ceram. Int.* 527-532 (2003).
9. B. Li-G. Williams, S. C. Rand, T. Himklen and R. M. Laine. Continuous-wave ultraviolet laser action in strongly scattering Nd-doped alumina. *Opt. Lett.* 27, 6, 394-396 (2002).
10. J. Subrt, J. Bohacek, V. Stengl, T. Grygar, P. Bezdecka. Uniform particles with a large surface area formed by hydrolysis of $\text{Fe}_2(\text{SO}_4)_3$ with urea. *Mater. Res. Bull.* 34, 6, 905-914 (1999).
11. T. Hernández, C. Bautista, P. Martín. Synthesis and thermal evolution of Mn-doped alumina nanoparticles by homogeneous precipitation with urea. *Mater. Chem. Phys.* 92, 366-372 (2005).
12. I. G. Serradilla, A. Calleja, X. C. Capdevila, M. Segara, E. Mendoza, J. Teva, X. Granados, X. Obradors, F. Spiell. Synthesizing the Y-123/Y-211 composite by the PVA method. *Supercond. Sci. Tech.* 15, 566-570 (2002).
13. H. J. Kweon, G. B. Kim, H. S. Lim, S. S. Nam, D. G. Park. Synthesis of $\text{Li}_{0.85}\text{Ni}_{0.85}\text{Co}_{0.15}\text{O}_2$ by the PVA-precursor method and charge-discharge characteristics of a lithium ion battery using this material as cathode. *J. Power Sources.* 83, 84-88 (1999).
14. M. A. Gullgun, M. H. Nguyen. and W.M. Kriven. Polymerized organic-inorganic synthesis of mixed oxides. *J. Am. Ceram. Soc.* 82, 3, 556-560 (1999).
15. P. Tarte. Infra-red spectra of inorganic aluminates and characteristic vibrational frequencies of AlO_4 tetrahedra and AlO_6 octahedra. *Spectrochim. Acta A23*, 2127-2132 (1967).
16. R. L. Frost, J.T. Kloppe, J.L. and Szety. Dehydroxylation and the vibrational spectroscopy of aluminum (oxo)hydroxides using infrared emission spectroscopy part III: diaspor. *Appl. Spectrosc.* 53, 829-835 (1999).
17. S-J Lee, S-Y Chun, C-H Lee and Y-S Yoon. Fabrication of nanosized alumina powders by a simple polymer solution route. *J. Nanosci. Nanotechnol.* 6, 3633-3636 (2006).
18. P. Duran, F. Capel, D. Gutierrez, J.I. Tartaj, C. Moure. Cerium (IV) oxide synthesis and sinterable powders prepared by the polymeric organic complex solution method. *J. Eur. Ceram. Soc.* 22, 9-10, 1711-1721 (2002).

Recibido: 24.06.08

Aceptado: 21.08.08

